

General Disclaimer

One or more of the Following Statements may affect this Document

- This document has been reproduced from the best copy furnished by the organizational source. It is being released in the interest of making available as much information as possible.
- This document may contain data, which exceeds the sheet parameters. It was furnished in this condition by the organizational source and is the best copy available.
- This document may contain tone-on-tone or color graphs, charts and/or pictures, which have been reproduced in black and white.
- This document is paginated as submitted by the original source.
- Portions of this document are not fully legible due to the historical nature of some of the material. However, it is the best reproduction available from the original submission.

Final Report

To

**NATIONAL AERONAUTICS AND SPACE ADMINISTRATION
GODDARD SPACE FLIGHT CENTER, GREENBELT, MARYLAND 20771**

On

**The Application of An Optical Fourier Spectrum Analyzer On
Detecting Defects In Mass-Produced Satellite Photographs**

By

**Ravi Athale and Sing H. Lee
Department of Applied Physics & Information Science
University of California, San Diego
La Jolla, California 92093**

June 21, 1976

Work performed under contract

NGR-5-9-260

N76-26444

**Unclassified
42332**



**(NASA-CR-148198) THE APPLICATION OF AN
OPTICAL FOURIER SPECTRUM ANALYZER ON
DETECTING DEFECTS IN MASS-PRODUCED SATELLITE
PHOTOGRAPHS Final Report (California Univ.)
48 p HC \$4.00**

CSCI 14E G3/35

TABLE OF CONTENTS

	<u>Page</u>
ABSTRACT	1
I. INTRODUCTION.	2
II. Fourier Spectrum Analyzer	2
III. Experimental Results.	3
A. EBR Related Defects	3
B. Horizontal Scratches in Mass Production	19
IV. Conclusions	34
V. Design of the Automated Defect Monitoring System.	35
REFERENCES	42

FIGURES

	<u>Page</u>
FIGURE 1 Optical System for Fourier Spectrum Analysis	4
2 The spatial filter for analysis of horizontal scratches.	20
3 The patterned photodetector.	36
4(a) The Automated Defect Monitoring System	37
4(b) The System Utilizing a Beam-Splitter & Two Photodetectors. .	38
4(c) The mask to be inserted in the collimated beam	39
4(d) The spatial filter to be inserted in front of the photo-detector	39
5 The Control Unit	40

EXAMPLES

		<u>Page</u>
EXAMPLE 1(a)	Excessive Bit Slip.	5
1(b)	Bit Slip.	6
1(c)	Bit Slip Distributed Irregularly Throughout the Frame	7
1(d)	Line Test Pattern (a)	8
2	EBRIC Breakup Causing Loss of Image	9
3	Disabled Track at the Bottom of the Imagery	10
4	Synchronous Loss <u>Without</u> Blurring of Image.	11
5(a)	Density Variation	12
5(b)	Line Test Pattern (b)	13
6	Density Variation and Bit Slip.	14
7	Pin Hole.	15
8	Annotation Error.	16
9	Synchronous Loss <u>With</u> Blurring of Image	17
10	Missing Image in the Beginning of Work Order.	18

FRAMES

FRAME NO. 0001	21
0003	22
0006	23
0009	24
0012	25
0015	26
0020	27
0024	28
0028	29
0032	30
0037	31
0039	32
0040	33

ABSTRACT

A study is made on utilizing Fourier spectrum analysis to detect various defects in mass-produced pictures transmitted to earth from a satellite. A number of commonly encountered EBR related defects are investigated. It is found that the following defects are readily detectable via Fourier spectrum analysis: (1) Bit Slip, (2) EBRIC breakup causing loss of image, (3) Disabled track at the top of the imagery. The scratches made on the film during mass production, which are difficult to detect by visual observation, also show themselves readily in Fourier spectrum analysis. A relation is established between the number of scratches, their width and depth and the intensity of their Fourier spectra. Other defects that are found to be equally suitable for Fourier spectrum analysis or visual (image analysis) detection are: (1) Synchronous loss without blurring of image, (2) Density variation in gray scale. The Fourier spectrum analysis is found to be unsuitable for detection of the following defects: (1) Pin holes, (2) Annotation error, (3) Synchronous loss with blurring of images, (4) Missing image in the beginning of the work order. At the end of this report, the design of an automated, real time system, which will reject defective films, is provided.

I. INTRODUCTION.

The number of pictures transmitted from satellite to receiving stations on earth is rapidly increasing. Into these pictures, certain defects are introduced in the course of their transmission to earth and their mass production. Presently human operators are employed to monitor the defective pictures. This method is expensive and at times not reliable enough, especially when dealing with a large number of pictures. In this report the result of our study on the utilization of Fourier spectrum analysis to monitor the defective pictures is presented. To begin the report, the basic optical Fourier spectrum analyzer is described. Then experimental results on the detection of defects using Fourier spectrum analysis are presented along with a brief explanation for each type of defect. At the end of this report, a design for the automated monitoring system is provided.

II. Fourier Spectrum Analyzer.

When a transparency is placed in front of a convex (Fourier transforming) lens and illuminated with collimated monochromatic light, the Fourier transform of that transparency is obtained in the back focal plane of the lens. The following equation gives the relation between i) the position (x,y) in the back focal plane (Fourier plane), ii) the spatial frequency (u,v) at that point (x,y), iii) the wavelength of illumination (λ) and iv) the focal length (f) of the convex lens¹:

$$u = \frac{x}{\lambda f}, \quad v = \frac{y}{\lambda f}.$$

Physically, different spatial frequencies (u, v) correspond to plane waves travelling at different angles with respect to the optical axis. Any image can be decomposed into a collection of plane waves with different intensities travelling at various angles with respect to the optical axis. Thus the Fourier spectrum of an image gives an indication of the intensities of the different plane waves (which corresponds to the structural composition of the image) that make up the image.

The optical system used for Fourier spectrum analysis of the defective film is shown in Figure 1. The output of the Spectra-Physics He-Ne laser (5 mW, Model 134) was filtered by a 20X microscope objective and a 5 μ m size pin hole (Jodon Engineering). The filtered beam was collimated using a convex lens (C). The film to be examined was illuminated by the collimated beam and was placed in front of the Fourier transforming lens (Schneider 30 cm. focal length lens). The back focal plane of this lens contained the Fourier spectrum of the film, which was then magnified by a Bausch-Lomb 9 inch focal length lens (M) and was imaged onto the recording film (Kodak high contrast copy film) in a camera.

The ability of optical Fourier spectrum analyzer to monitor films with certain defects derives primarily from the fact that the spectral components contributed by these defects are distinct from those contributed by a good satellite picture, as demonstrated by the following experimental results.

III. Experimental Results.

A. EBR Related Defects:

In this section experimental results on satellite imageries with EBR related defect examples are presented. The Fourier spectra were all recorded on Kodak high contrast copy film (to bring out the weak signals clearly), with the same exposure time of 1 sec.

It is found that the following defects are readily detectable via Fourier spectrum analysis: 1) Bit slip, 2) EBRIC breakup causing loss of image, 3) Disabled track at the top of the image. Additional defects which are prominent in Fourier plane as well as image plane are listed below: 1) Synchronous loss without blurring of image, 2) Density variation in gray scale. The contributions of the following defects to the Fourier spectra are diffuse and not distinct from the Fourier spectra of the pictures, making their detection by Fourier spectrum analysis difficult: 1) Pin holes, 2) Annotation error, 3) Synchronous loss with blurring of image, 4) Missing image in the beginning of the work order.

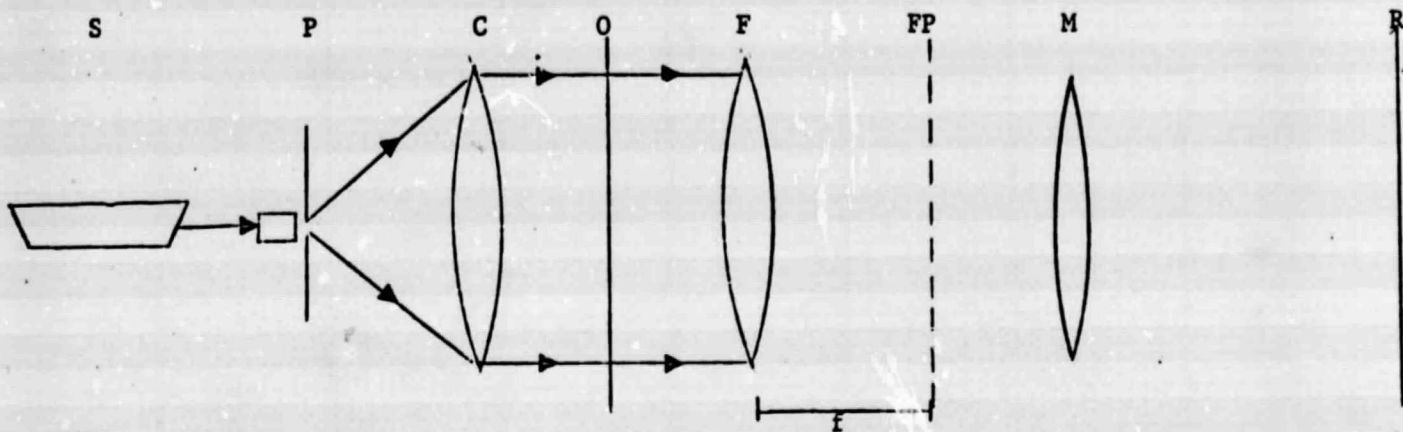


Figure 1: Optical System for Fourier Spectrum Analysis

S = Spectra-Physics He-Ne Laser.

P = Jodon Engineering microscope objective-pinhole assembly.

C = A convex collimating lens.

O = The film to be analyzed.

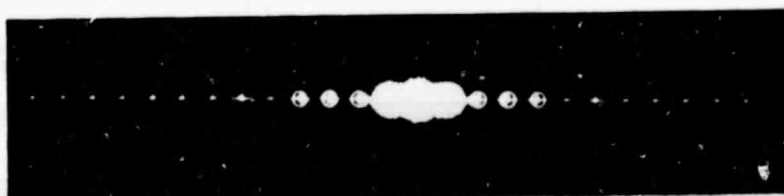
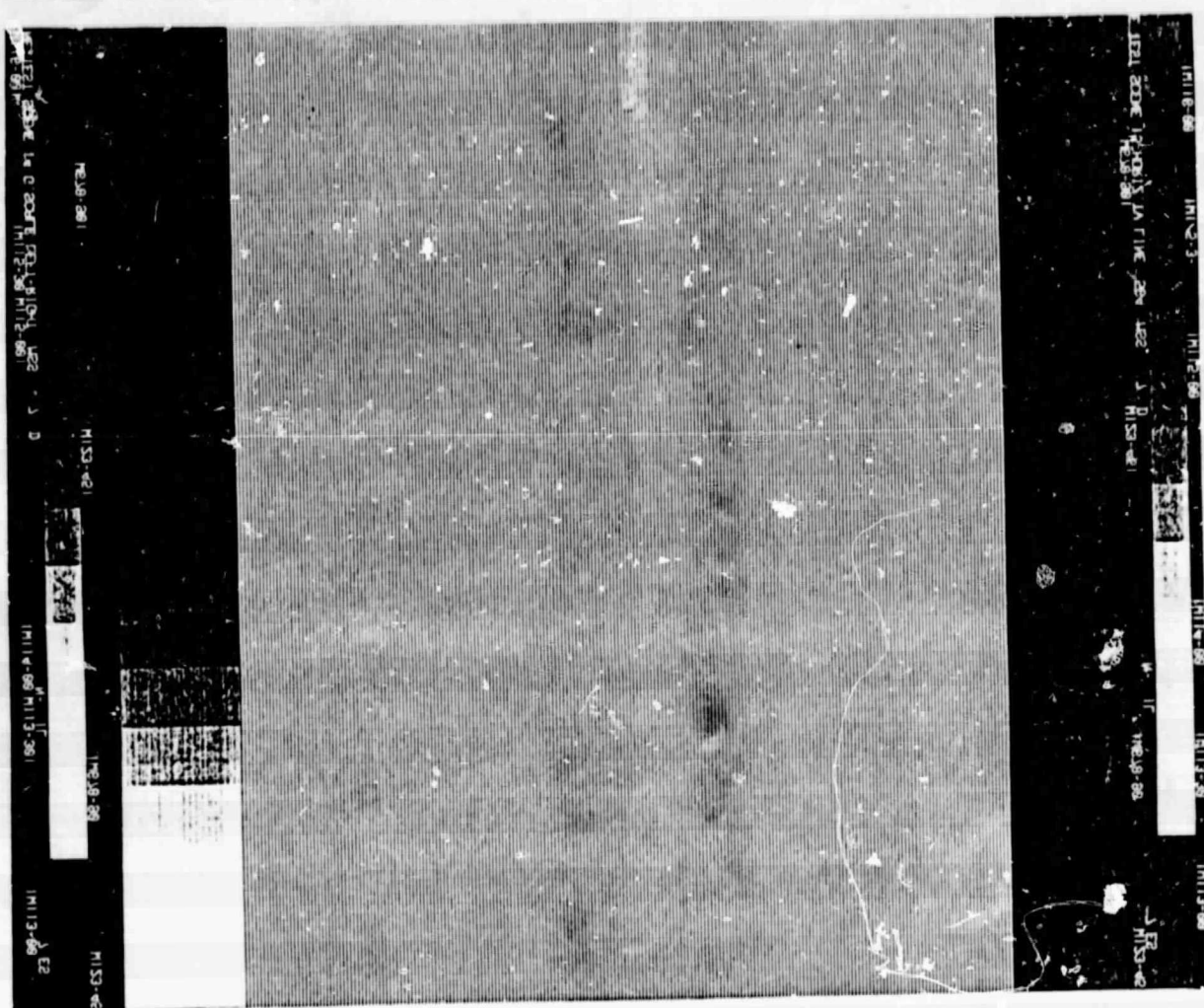
F = Fourier transforming lens (Schneider 30 c.m. focal length lens).

FP = Back focal plane (Fourier plane).

M = Magnifying lens (Bausch and Lomb 9 inch focal length lens).

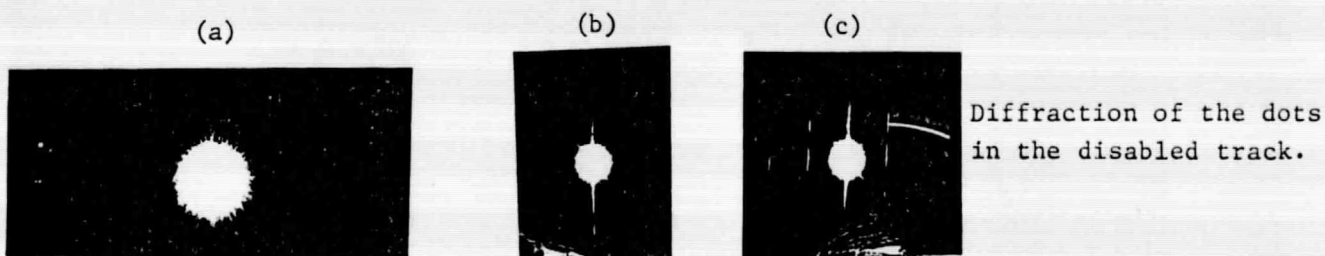
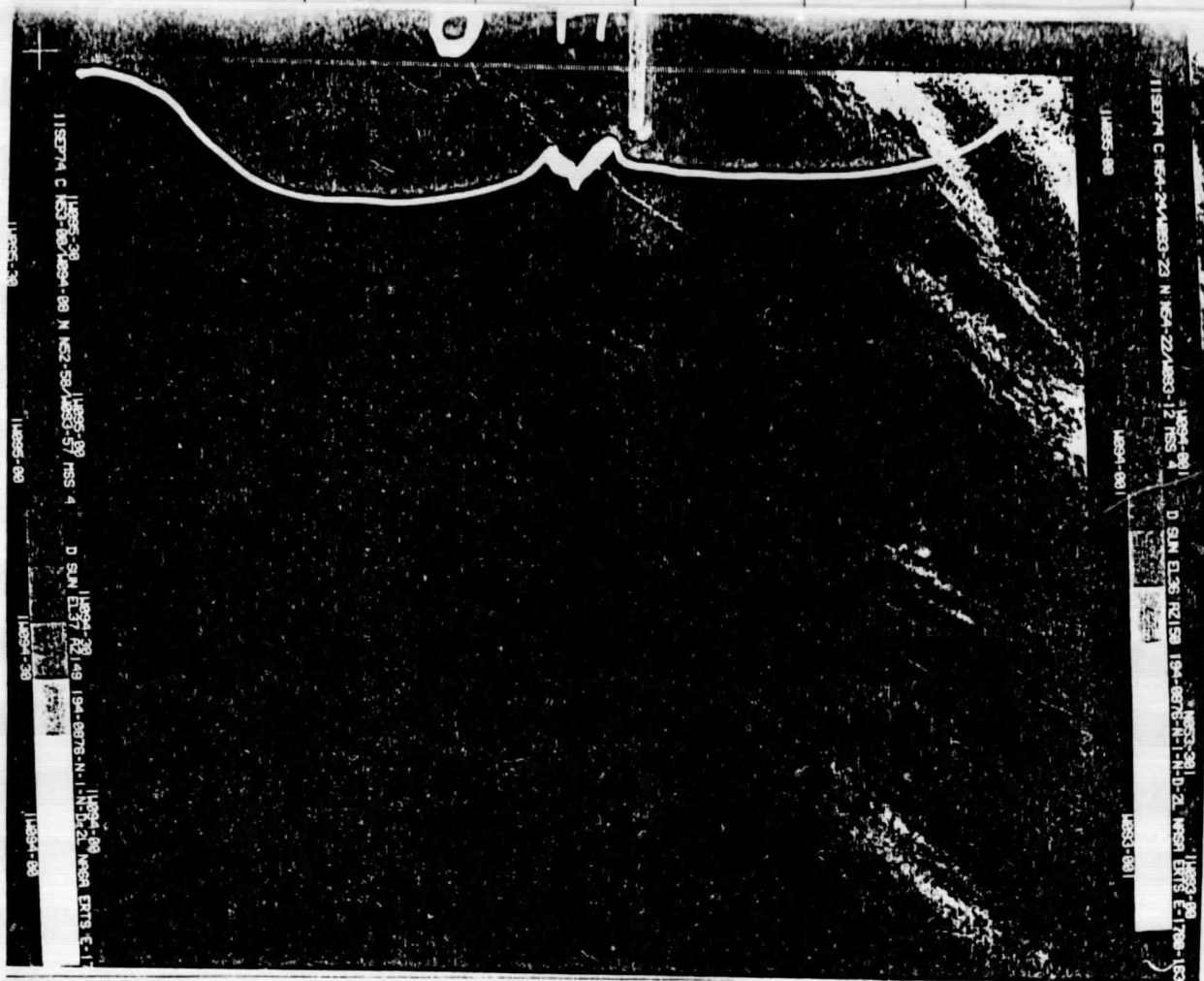
R = The recording photographic film (Kodak high contrast copy film).

f = Focal length of the Fourier transforming lens (30 c.m. in this case).



Example 1 (d): Line Test Pattern (a).

Explanation on Fourier Spectrum: The Fourier spectrum of the line test pattern is similar to that of a bit slip pattern except that it is much greater in intensity because the pattern on the film is much stronger.

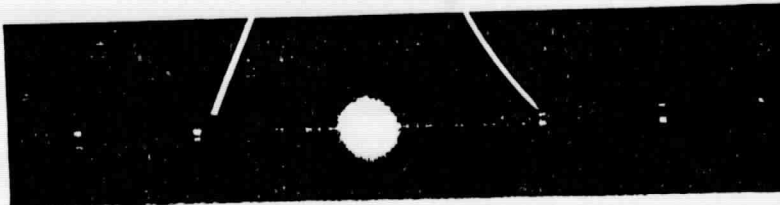


Example 3: Disabled Track at the Top of the Imagery.

Explanation on Fourier Spectrum: (a) Fourier spectrum of the entire image. Photographs (b) and (c) were taken when the top edge of the frame was illuminated through a slit. (b) is obtained when the frame is defective and (c) is obtained when the frame is normal. It is seen that although photograph (a) does not contain any distinct features indicating the defect, photograph (c) is clearly different from photograph (b) in the diffraction pattern generated by the dots in the disabled track. Hence, it is possible to detect the defect, if it is known a priori that the defect occurs only at the edges.

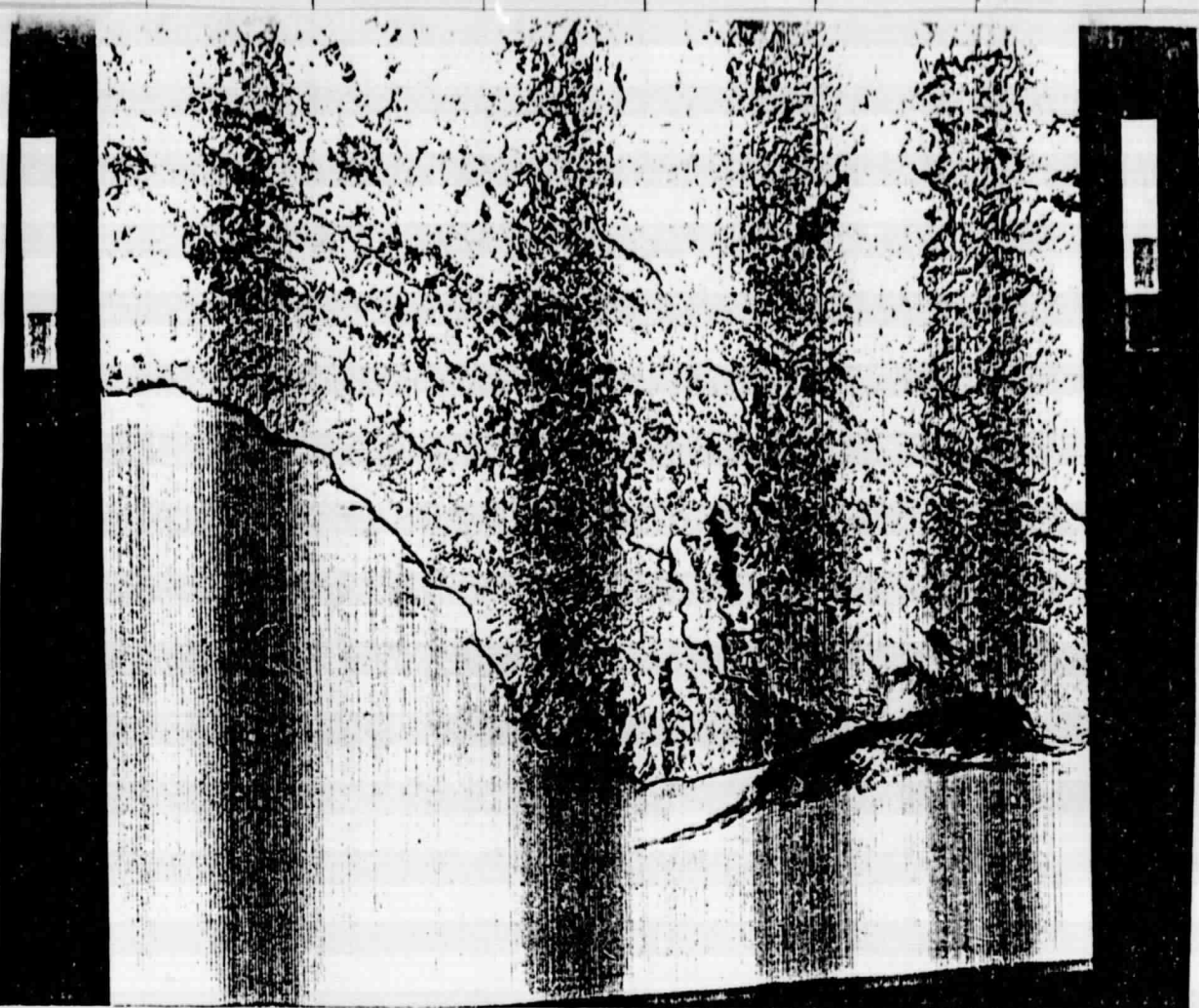


Note the two sets of
scan line spectrum.



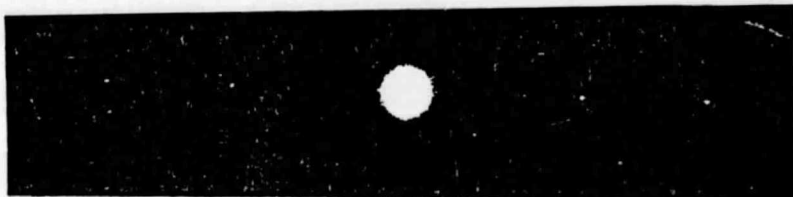
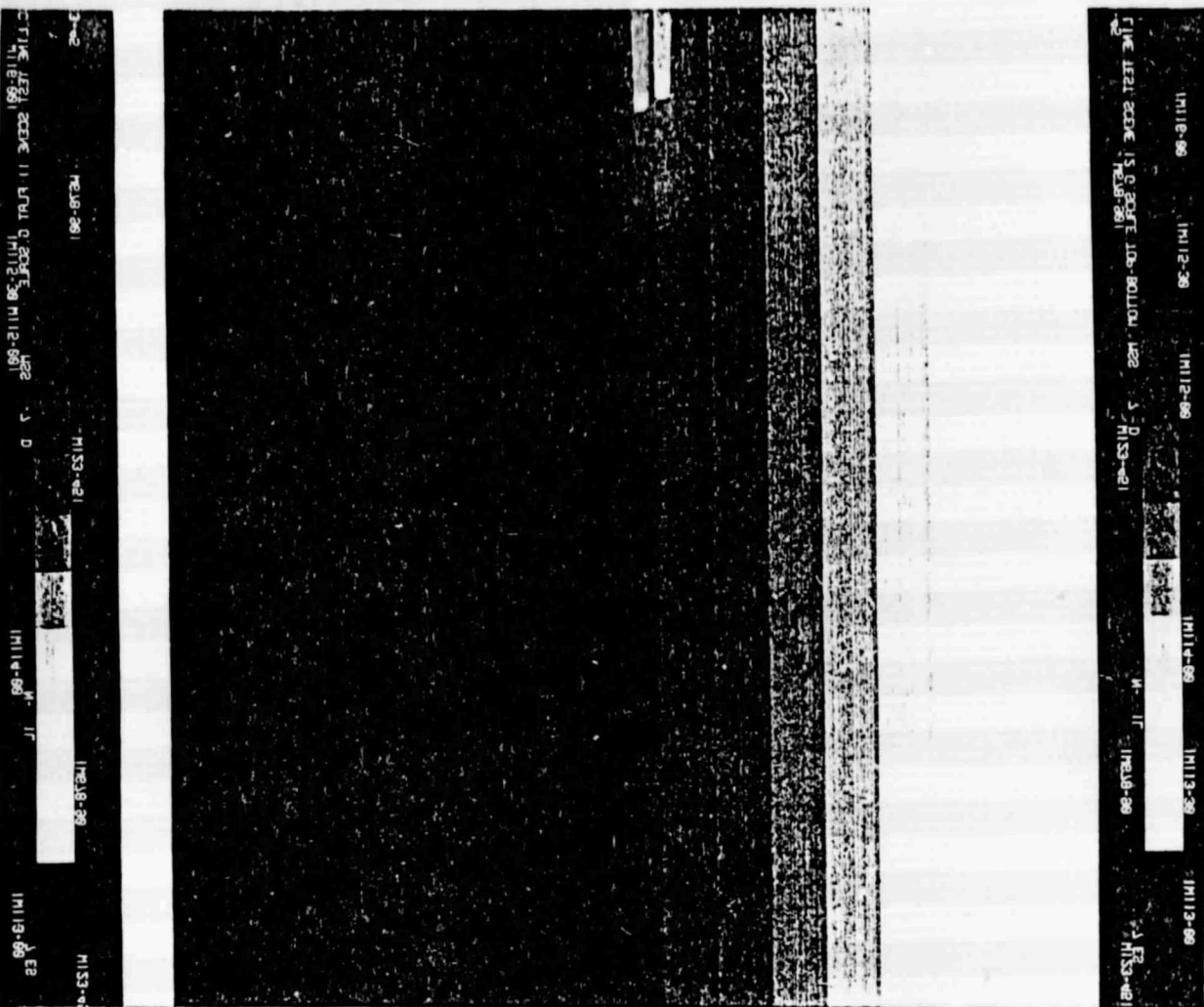
Example 4: Synchronous Loss Without Blurring of Image.

Explanation on Fourier Spectrum: There are two sets of scan line patterns in the Fourier spectrum. This implies that the frame must have been multiply exposed (with the sets of scan lines at an angle to each other). If this is always the case, this defect can be detected in the Fourier plane. Otherwise, spectral analysis cannot be utilized.



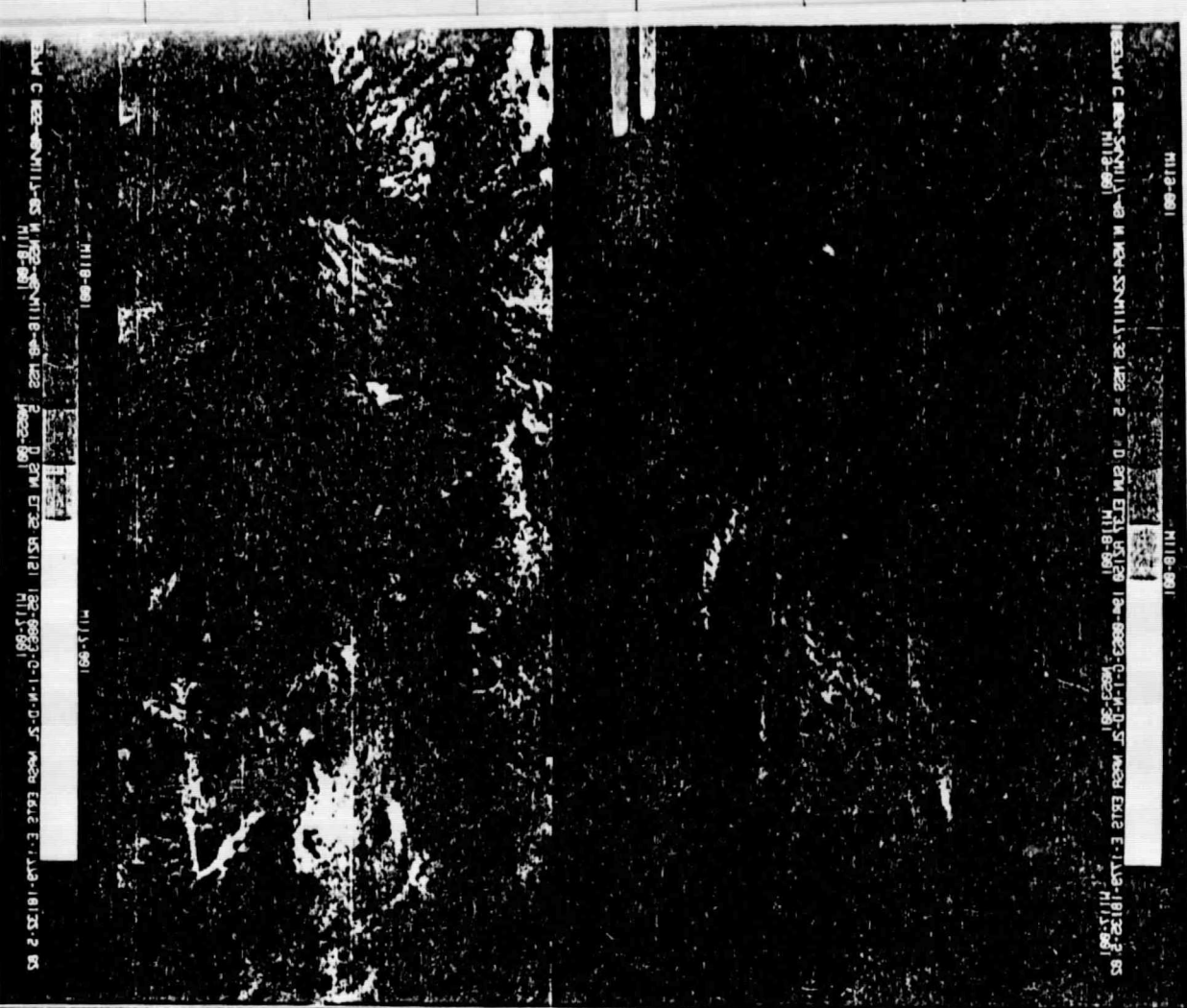
Example 5 (a): Density Variation.

Explanation on Fourier Spectrum. The alternate dark and light stripes behave like a crude and weak grating giving rise to the side extensions. The signal is quite weak in this case as the average transmittance of the picture is low.

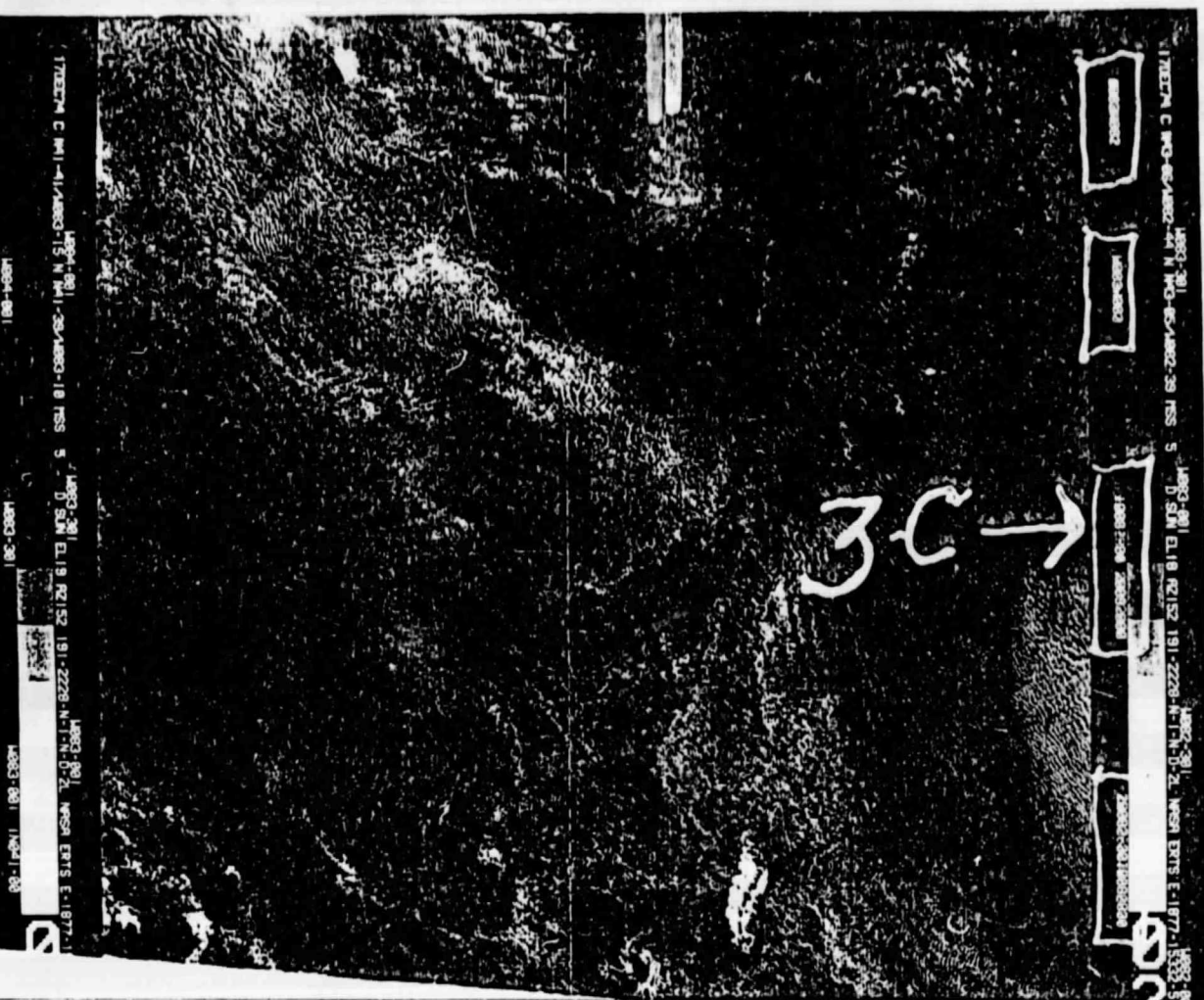


Example 5 (b): Line Test Pattern (b).

Explanation on Fourier Spectrum: This picture does not contain any other information except the grey scale, which is similar to the defect pattern in example 5 (a). The similarity in those two Fourier spectra is in the weak side-extensions. Thus we can associate the side extensions with the density variation pattern.



Example 6: Density Variation and Bit Slip.



Example 8: Annotation error.

Explanation on Fourier Spectrum: Annotation error is localized in the object plane; it is very difficult to be detected in the Fourier spectrum.



Example 9: Synchronous Loss With Blurring of Image.

Explanation on Fourier Spectrum: The effect of blurring in the image on its Fourier spectrum is a reduction in its high frequency contribution. Whether it is detectable or not depends on the variations in the high frequency content among different frames relative to the change produced by the blurring.



Example 10: Missing Image in the Beginning of Work Order.

B. Horizontal Scratches in Mass Production:

The Fourier spectra of horizontal scratches on the frames are narrow vertical lines. When a spatial filter shown in Figure 2 was placed in the Fourier plane, the Fourier spectra of the scratches were transmitted while blocking the Fourier spectra of the images. In the examples presented, the Fourier spectra of the pictures did diffract around the spatial filter to expose the film in the center. The filtered Fourier spectra were recorded on a photographic film (Kodak high contrast copy film) with exposure of 1 second.

To establish correlation between the Fourier spectra and important scratch parameters (such as the length, width and depth of the scratches) the frames were also examined under a calibrated magnifier. The experimental results are presented below. It is concluded from the results that the use of optical Fourier spectrum analyzer can be quite effective in detecting scratches on transparencies.

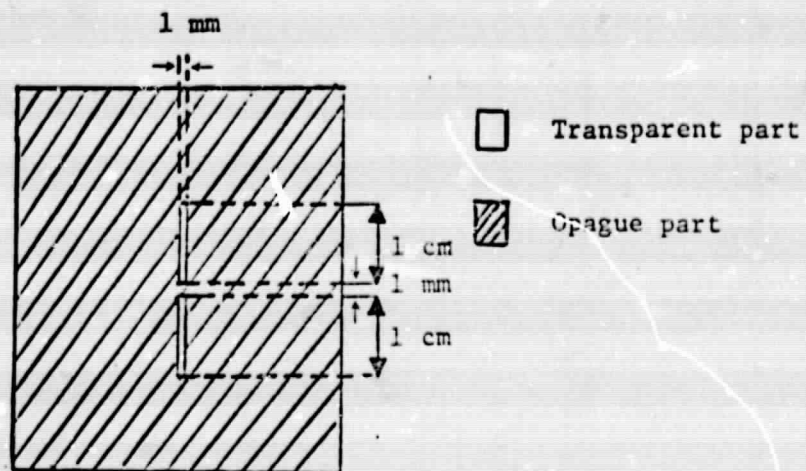
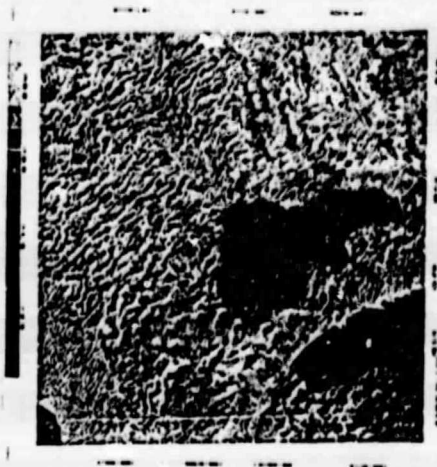
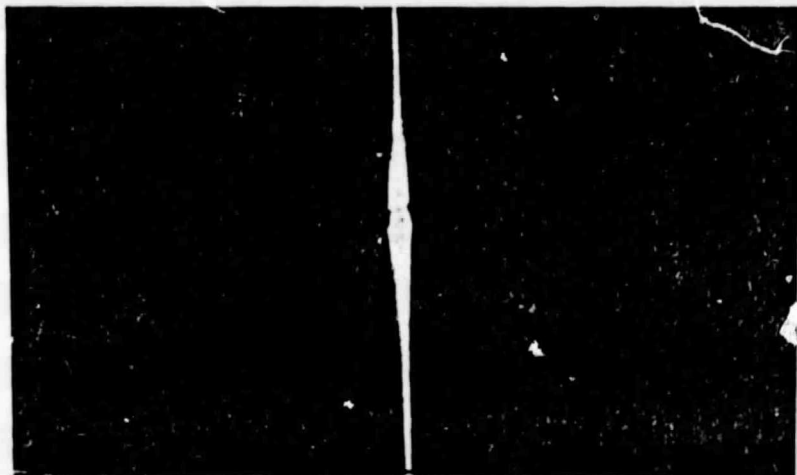


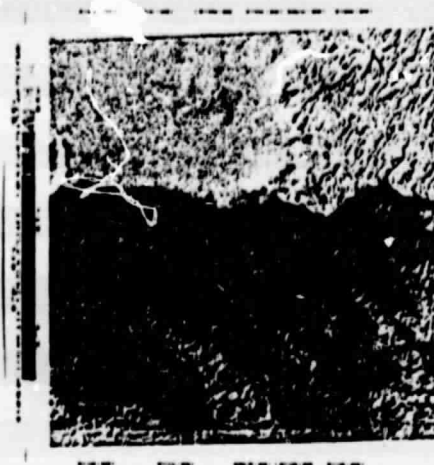
Figure 2. The spatial filter for analysis of horizontal scratches.



Frame No.: 0001

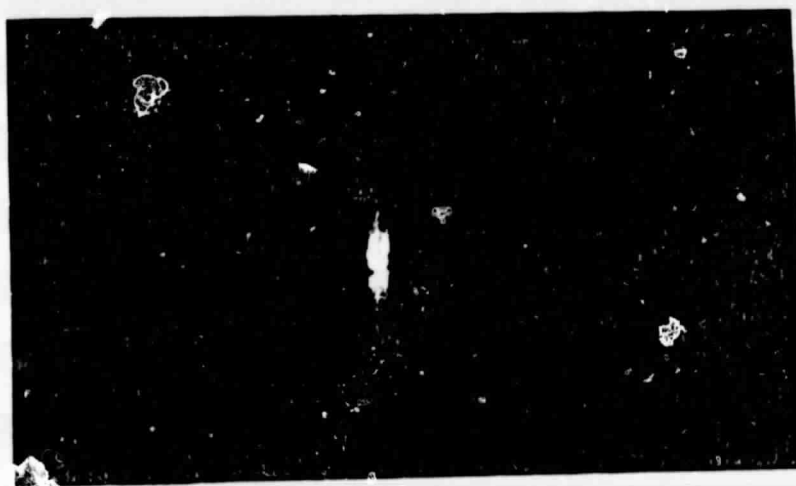
Description of scratches: One wide and deep scratch, and approximately fifteen thin and weak scratches. All the scratches run across the whole frame.





Frame No.: 0003

Description of scratches: Two weak and discontinuous scratches.

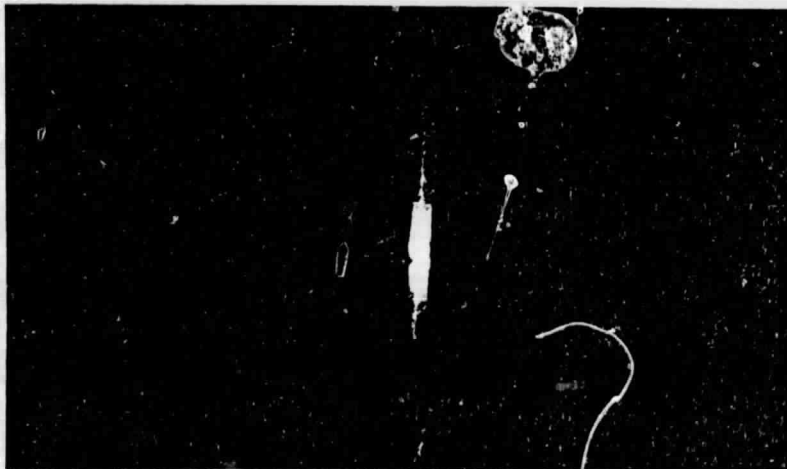


00006



Frame No.: 0006

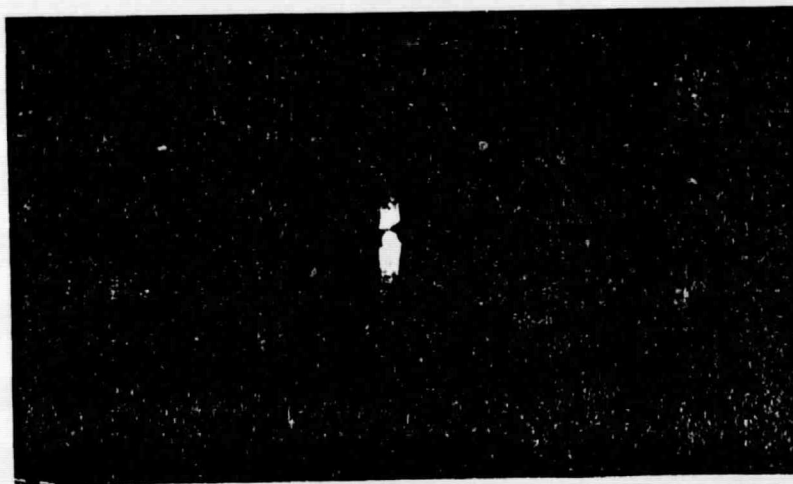
Description of scratches: One weak and continuous scratch at the top.
Two weak and discontinuous scratches in the middle.





Frame No.: 0009

Description of scratches: One weak and continuous scratch at the top of the frame, one weak and discontinuous scratch in the middle. The average transmittance of this frame is less than the previous frames.



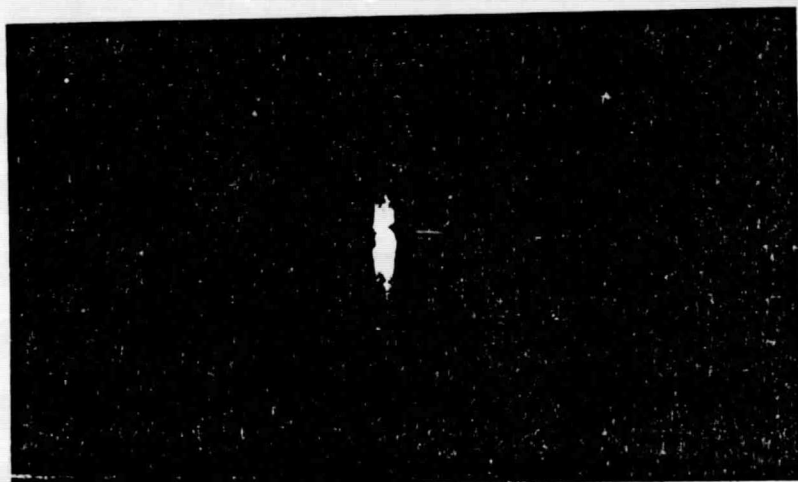
00012



Frame No.: 0012

Description of scratches: One weak and continuous scratch at the top.

A few very weak scratches and two wide and short (length 2mm.) scratches in the middle.

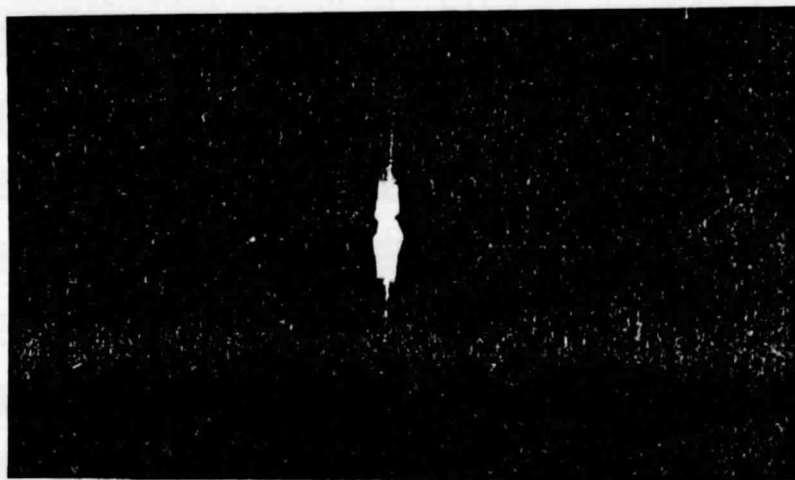


00015



Frame No.: 0015

Description of scratches: One deep and continuous scratch at the top. Three wide and short (1 to 4 mm. in length) scratches and a few very weak and continuous scratches distributed throughout the frame. The average transmittance of this frame is less than that of the other frames.

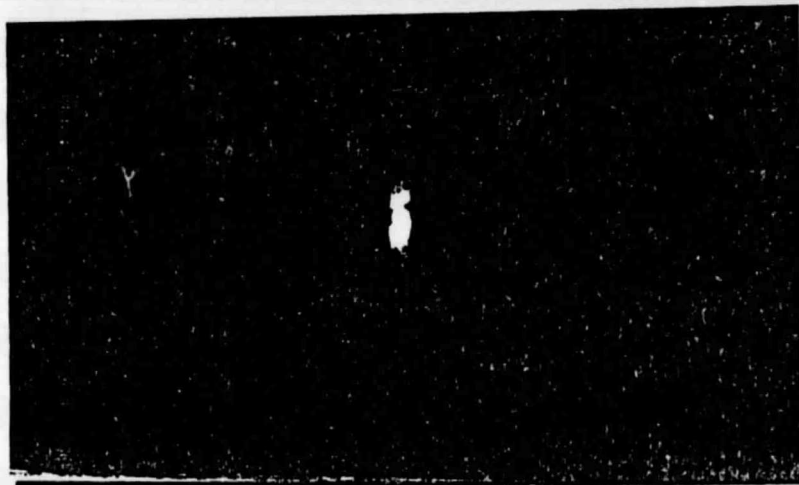


00020



Frame No.: 0020

Description of scratches: One weak and continuous scratch at the top and one in the middle. Two weak and short scratches distributed over the frame.

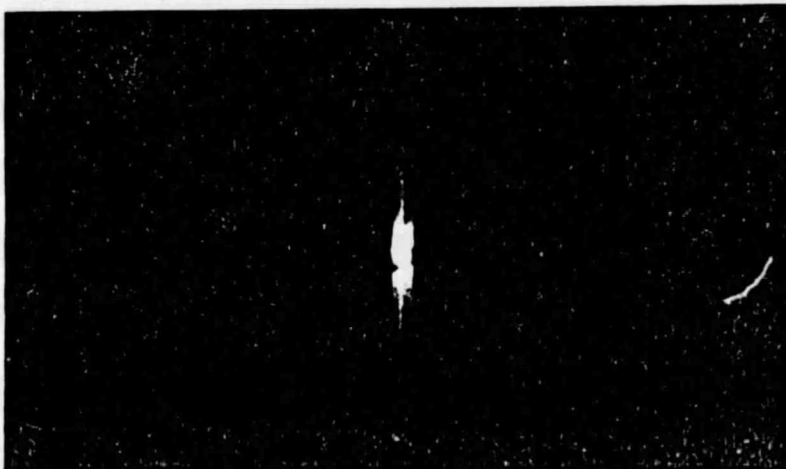


00024



Frame No.: 0024

Description of scratches: Three weak and continuous scratches in the middle and two wide and short (length of 3mm.) scratches in the corners.

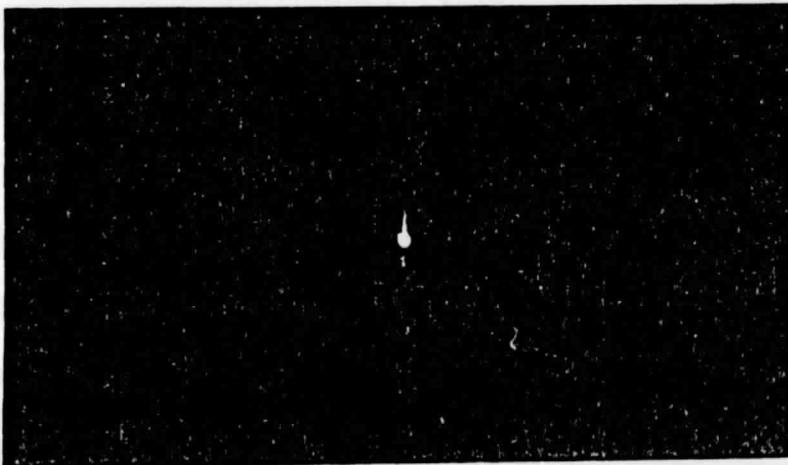


00028



Frame No.: 0028

Description of scratches: One weak and continuous scratch and a few discontinuous and very weak scratches. The average transmittance of this frame is much less than that of the other frames.

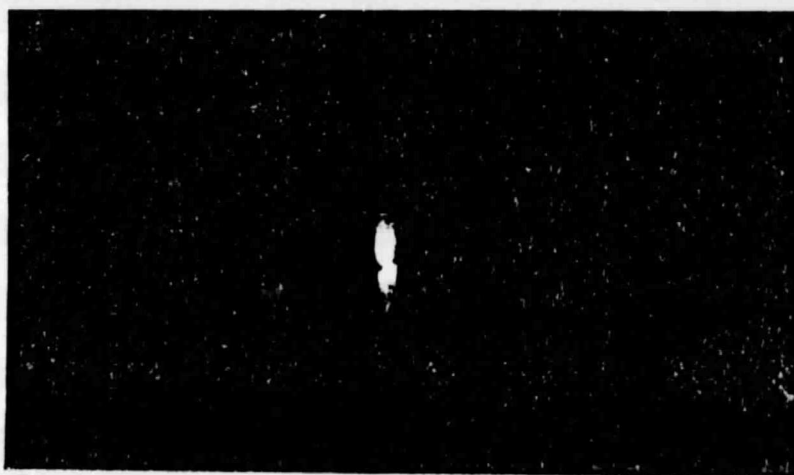


00032



Frame No.: 0032

Description of scratches: One weak and continuous scratch and one very weak and continuous scratch in the middle. One quite wide and short (length 2 mm.) scratch. The average transmittance of this frame is less than that of the other frames.

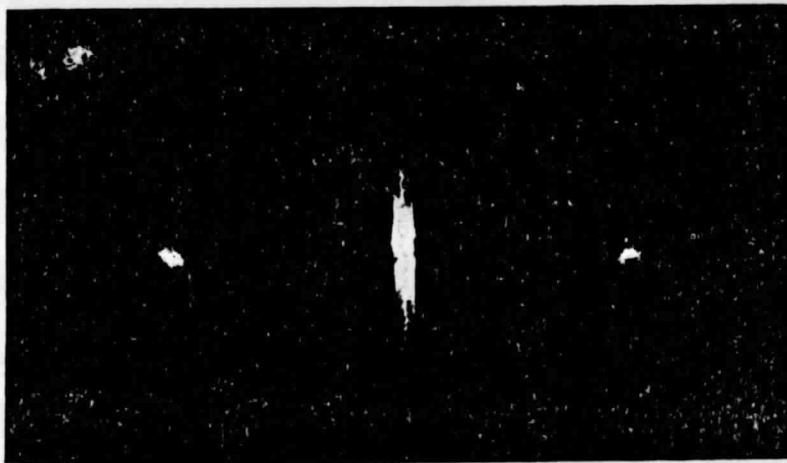


00037

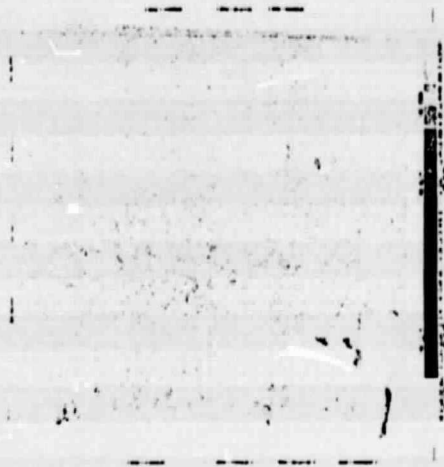


Frame No.: 0037

Description of scratches: Two weak and continuous scratches in the middle and two wide and short (2 to 3 mm. length) scratches, elsewhere in the frame.

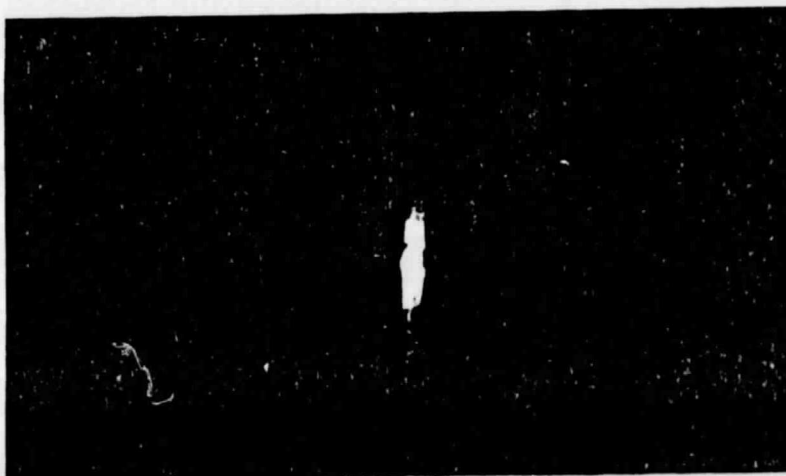


00039



Frame No.: 0039

Description of scratches: Two very weak and continuous scratches in the middle and two wide and short (2 to 3 mm. length) scratches elsewhere in the frame. The average transmittance of this frame is much more than that of the other frames.

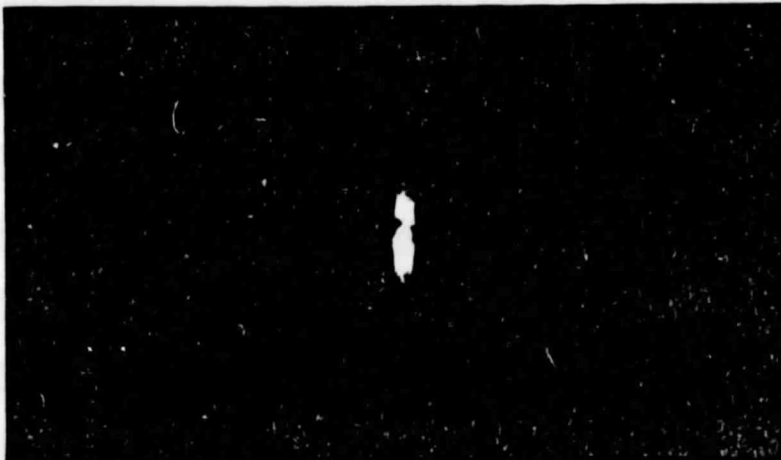


00040



Frame No.: 0040

Description of scratches: One very weak and continuous scratch in the middle. One very wide and deep scratch 1 mm. in length and two wide and short (length 2 and 3 mm.) scratches.



IV. Conclusions.

The experimental results indicate that the following defects could be detected by optical Fourier spectrum analyzer because these defects have some form of regularity and they contain spatial frequencies outside the spatial frequency domain of the picture:

1. Bit Slip
2. EBRIC breakup causing loss of image
3. Disabled track at the top of the image
4. Synchronous loss without blurring of image
5. Density variation in gray scale
6. Horizontal scratches made during mass production

The following defects are found to be unsuitable for Fourier spectrum analysis because they lack features of regularity and do not contain any detectable spatial frequencies outside the frequency domain of the picture:

1. Pin hole
2. Annotation error
3. Synchronous loss with blurring of image
4. Missing image in the beginning of the work order.

In the following section a design is given for constructing an automated defect monitoring system.

V. Design of the Automated Defect Monitoring System.

The experimental results presented in the previous sections suggest that some of the defects under consideration have Fourier components distinct from the Fourier spectra of the pictures free from those defects. It is also apparent that the Fourier components of the defects are confined to the region between the low frequency part containing Fourier spectra of good picture and the Fourier

components of the scan line pattern (In the setup used in the previous sections, this region is a circular annular region with outer diameter 19 mm and inner diameter 1 mm). The intensity in this region is the signal denoting the presence of a defect. This signal will have to be normalized with respect to the average transmittance of the frame under consideration. The information about the average transmittance is contained in the low frequency part in the Fourier plane. So, a photodetector shown in Figure 3 will be able to detect both the signals simultaneously and could be used in the defect monitoring system as shown in Figure 4(a). This photodetector could be fabricated by a process similar to the one described in Reference 2 for the fabrication of a wedge-ring detector. Alternatively, a system using a beam splitter and two photodetectors with appropriate spatial filters could perform the same tasks (Figure 4(b)).

The operation of this system will be quite similar to the setup used to obtain the data in the previous sections. The film to be examined passes over the reels in steps of one frame at a time. The patterned photodetector (shown in Figure 3) is placed in the Fourier plane. The outputs from the two regions of the photodetector are fed to a control box, details of which are shown in Figure 5. The output V_1 from region 1 of the photodetector corresponds to the intensity of the Fourier components caused by the defects and is directly related to the presence and strength of the defects. This output (V_1) has to be amplified by a factor n so that the criterion for the rejection of a frame becomes $nV_1 \geq V_2$ $\left(\frac{nV_1}{V_2} \geq 1 \right)$ where V_2 is the output from region 2 corresponding to the average transmittance of the frame. This operation will be performed by a threshold device (e.g. a Zener diode) whose threshold is set by V_2 . The output of the threshold device is non-zero if and only if nV_1 is greater than V_2 as shown in Figure 5. This output of the threshold device triggers a warning device indicating a defective frame. The amplification factor depends on the particular setup used and has to be set so that the criterion for rejection is satisfied by

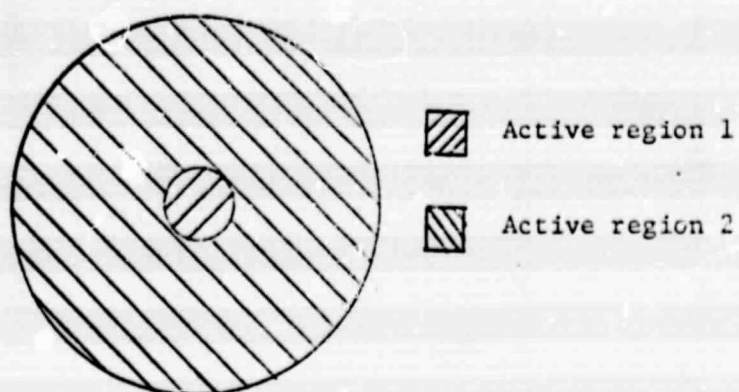


Figure 3. The patterned photodetector.

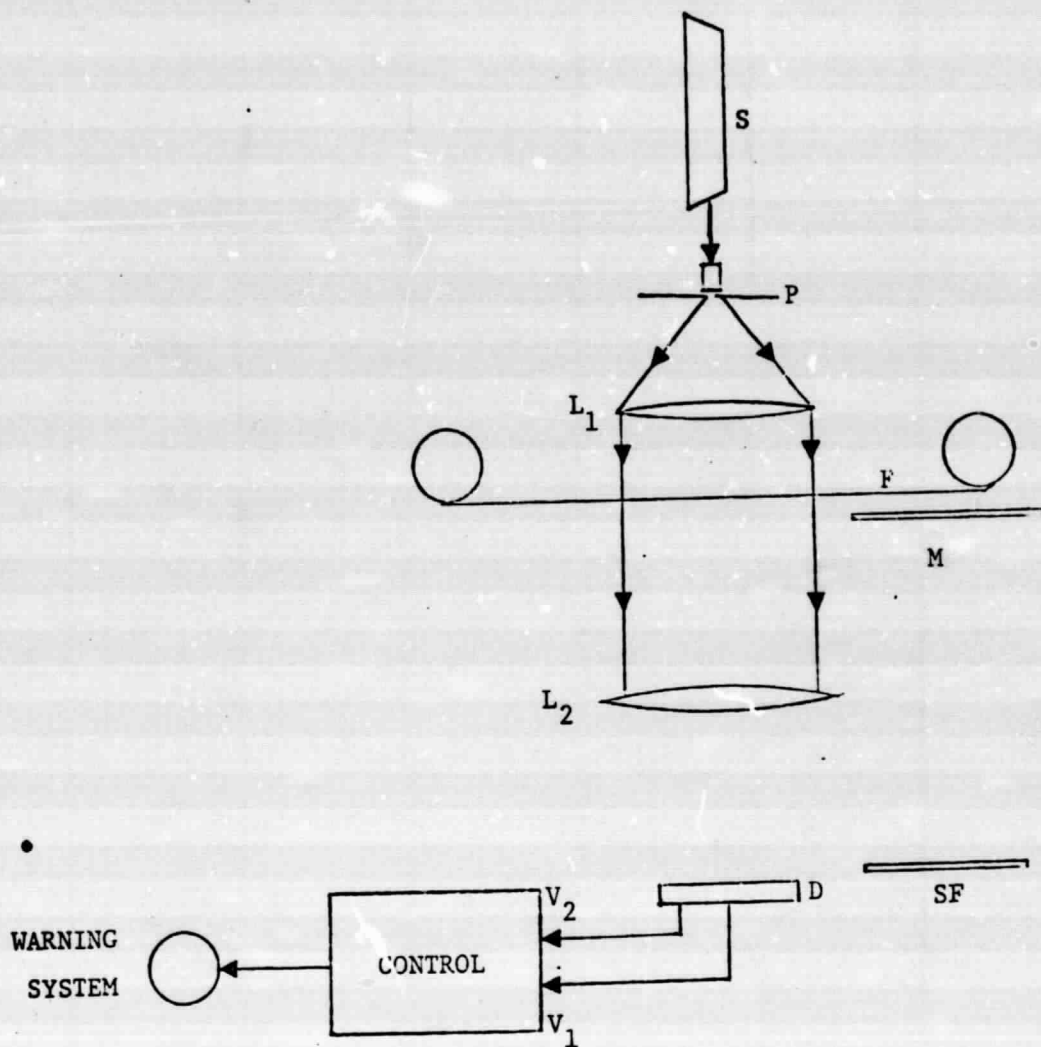


Figure 4 (a). The Automated Defect Monitoring System.

S = Laser source.

F = Film.

P = Pinhole spatial filter.

L_2 = Fourier Transforming Lens.

L_1 = Collimating lens.

SF = Spatial Filter (as shown in Figure 4(d)).

M = Mask (as shown in Figure 4(c)).

D = Patterned photodetector (as shown in Figure 3).

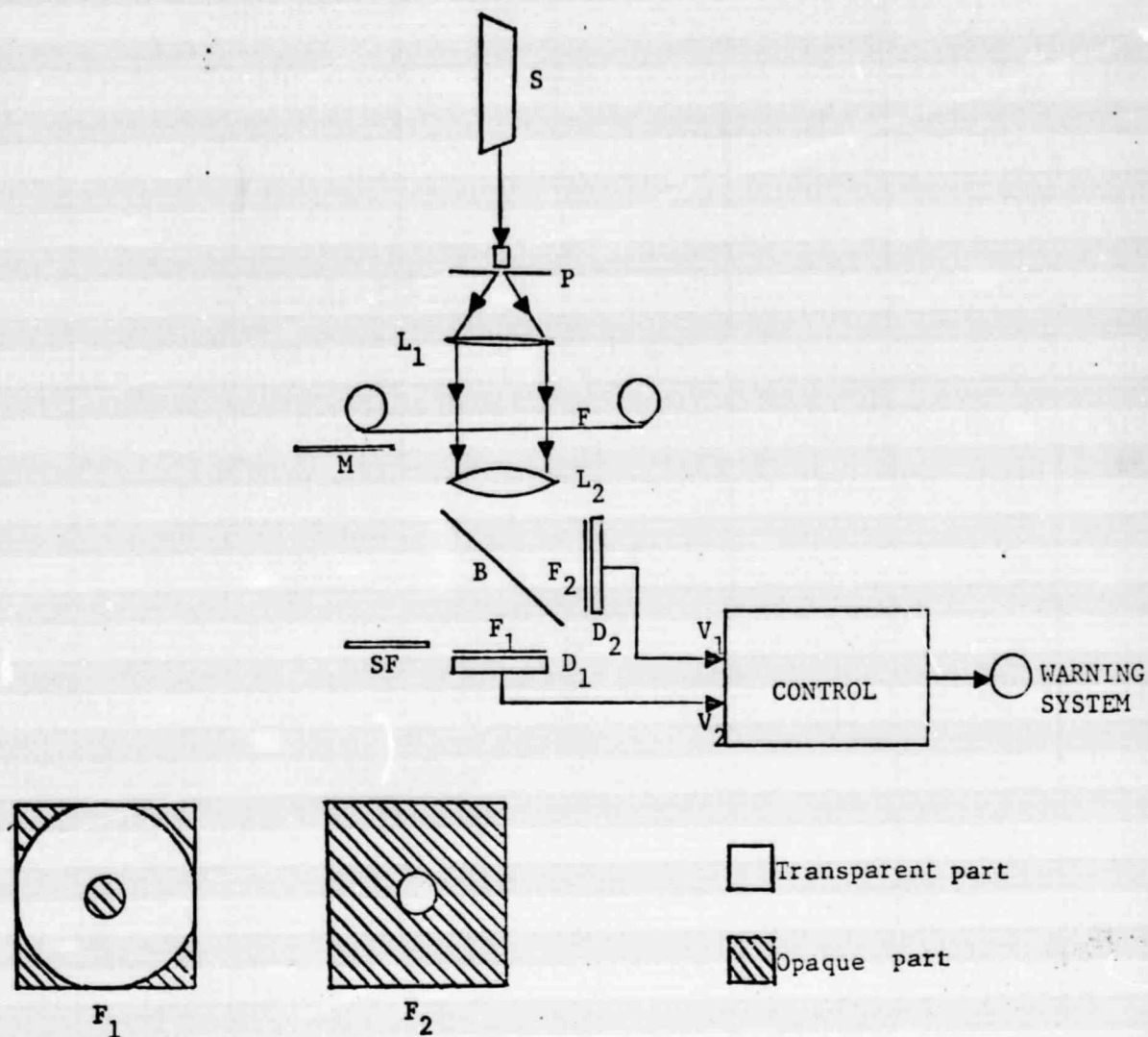


Figure 4 (b). The System Utilizing a Beam-Splitter & Two Photodetectors.

S = Laser source.

P = Pinhole spatial filter.

L₁ = Collimating lens.

M = Mask (as shown in Figure 4(c)).

F = Film.

L₂ = Fourier Transforming lens.

B = Beam-splitter

F₁ & F₂ = Spatial filters as shown.

D₁ & D₂ = Photodetectors.

SF = Spatial filter (as shown in Figure 4(d)).

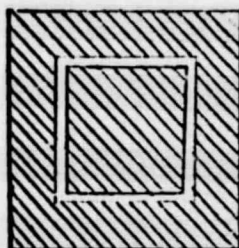


Figure 4(c). The mask to be inserted in the collimated beam.

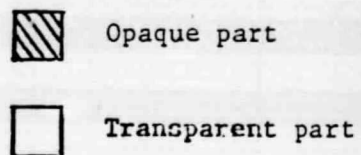
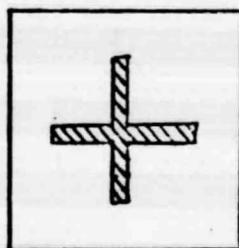


Figure 4(d). The spatial filtered to be inserted in front of the photodetector.

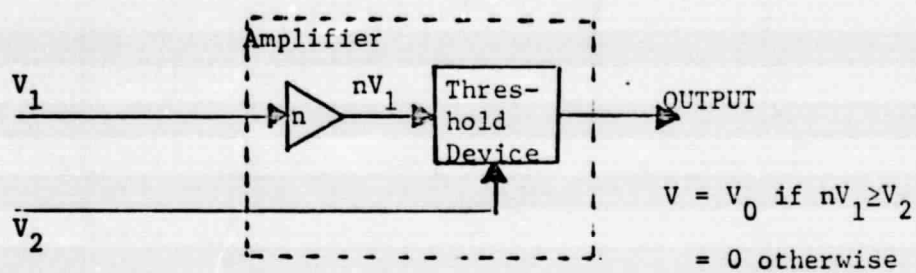


Figure 5. The Control Unit.

the weakest signal corresponding to a rejectable defect.

In order to detect a disabled track on the edges of the frame it was determined in Section III. A that it will be necessary to illuminate the frame only on the edges. For this case a mask shown in Figure 4(c) is inserted in the collimated beam and a filter shown in Figure 4(d) is inserted in front of the detector to eliminate the Fourier components of the mask. Now the output V_1 suggests presence of disabled tracks on the edges. The filter shown in Figure 4(d) blocks region 2 of the detector (as well as the diffraction pattern of the mask) making V_2 zero. The presence of signal V_1 will thus activate the warning device causing the rejection of the frame.

The system described above is totally automated with operator control coming only in insertion of the mask and the filter. The decision making is now to be done electronically and will be considerably more reliable and faster than the system utilizing human operators.

References

- [1] A.R. Shulman, "Optical Data Processing," Chapter 5 (Wiley - Interscience Publication, 1970).
- [2] N. George, H.L. Masdan, "Diffraction pattern sampling for pattern recognition and metrology", p. 494. Proceedings of the Electro-optical Systems Design Conference--1975, Anaheim, California.